Self-Synchronization of Laser Modes and Multistability in Quantum Cascade Lasers

Aleksander K. Wójcik,[1] Nanfang Yu,[2] Laurent Diehl,[2] Federico Capasso,[2] and Alexey Belyanin[1,*]
[1]*Department of Physics and Astronomy, Texas A&M University, College Station, Texas, 77843 USA*
[2]*School of Engineering and Applied Sciences, Harvard University, Cambridge, Massachusetts, 02138 USA*
(Received 3 September 2010; revised manuscript received 24 February 2011; published 1 April 2011)

We predict and confirm experimentally the regime of complete synchronization between lateral modes in a quantum cascade laser, when frequency combs belonging to different lateral modes merge into a single comb. The synchronization occurs through the transition from multistability to a single stable state and is accompanied by phase locking and beam steering effects.

DOI: 10.1103/PhysRevLett.106.133902 PACS numbers: 42.55.Px, 05.45.Xt, 42.65.Pc

Synchronization in an ensemble of weakly coupled oscillators is one of the most fascinating and universal phenomena in nature [1]. It has been observed and studied in a vast variety of systems: from lasers and nonlinear optical systems to chemical reactions, neurons, and genetic circuits; see, e.g., [2–6] and references therein. Synchronization results in phase coupling and frequency locking of initially incoherent oscillations with random relative phases. Thus, a macroscopic coherent state emerges, either spontaneously or under periodic forcing.

In lasers, elementary oscillators are eigenmodes of a laser cavity. Nonlinear phase coupling between longitudinal cavity modes plays a prominent role in nearly all types of lasers and leads to generation of ultrashort pulses. One notable exception is quantum cascade lasers (QCLs) where the gain recovery time (of the order of 1 ps) is much shorter than the cavity roundtrip time and the photon lifetime (a class A laser [7], the only solid-state laser in this class). This leads to a strong damping of any perturbation of light intensity in a cavity, except maybe in the fully coherent regime when the time scale of Rabi oscillations becomes shorter than the dephasing time of the optical polarization; see [8,9]. Although in recent work [10] active mode locking by gain modulation has been demonstrated near laser threshold, passive mode locking remains an elusive goal. Surprisingly, in a recent study [11] we found that the phases of different *transverse* modes can be spontaneously coupled in a standard QCL even without a saturable absorber or any other nonlinear element in a cavity, except the nonlinearity of the gain transition. In the present work we report an ''ultimate'' phase-locking regime of complete synchronization when combs of longitudinal modes belonging to different lateral modes merge into a single comb.

Phase coupling of transverse modes in lasers has been extensively studied before, with the most recent surge of interest to this topic stimulated by applications in communications and optical information processing (chaos synchronization, control of pattern formation, spatial and polarization entanglement), see, e.g., [2,12–14]. However, synchronization was achieved previously by periodic modulation of laser parameters or external or mutual optical coupling. Our present finding shows that synchronization in QCLs is possible without any stabilizing elements, likely due to the combination of strong nonlinearity associated with intersubband laser transitions and overdamped relaxation oscillations. Thus studies of modal phase coherence in QCLs add new dimension to this actively developing field and open up new applications in the midinfrared and terahertz range, such as beam control and combining, electrical or optical switching or modulation, and free space communications; see, e.g., [15–19].

An experimental example of synchronization is presented in Fig. 1, which corresponds to a buried-heterostructure laser fabricated by Hamamatsu, with an active region width of 19.4 μm. Starting from threshold, this laser operates on three lateral modes TM_{00}, TM_{01}, and TM_{02}, and its far field is well described by an incoherent addition of modal intensities. The spectrum consists of three distinct combs

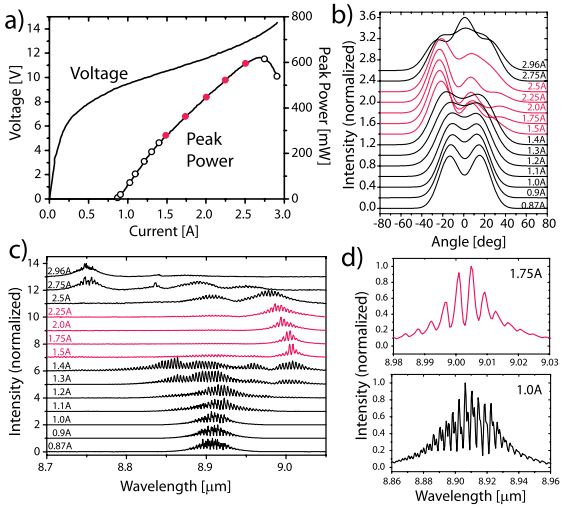

FIG. 1 (color online). Laser measurements in the pulsed regime with different stability regions marked with different colors. (a) LIV curve. (b) Far-field measurements. (c) Spectra measurements. (d) close-up view of the spectra at two values of current.

of longitudinal modes, each comb belonging to a different lateral mode. At about 1.5 A, both the spectrum and the far field undergo a drastic change. The spectral combs merge into a single comb [Figs. 1(c) and 1(d)], as if only one lateral mode were present. At the same time, the far-field pattern becomes very asymmetric and shifts by about 30 degrees off the waveguide axis [Fig. 1(b)]. This far-field indicates the presence of all three lateral modes. Moreover, it can only be fitted by a *coherent* addition of the fields of all three lateral modes with fixed mutual phases. These experimental findings cannot be explained by thermal distortion of the far field because the laser was operated in the pulsed regime with low duty cycle and there is clear correlation between the far field and spectral changes. We also note that the synchronization regime exists within a certain range of currents and its onset or disappearance with changing current are quite sharp, whereas thermo-optical effects are expected to appear gradually and become more pronounced with increasing current.

This frequency-synchronized, phase-coherent behavior persists over a wide range of currents and is reproducible. Then at about 2.75 A, the laser undergoes the transition back to an unlocked state with several distinct spectral combs and symmetric far-field pattern that can be fitted by incoherent addition of lateral mode intensities.

We observed synchronization in devices of different wavelengths and waveguide widths, fabricated by different manufacturers. The only common property was that all devices were of buried-heterostructure type, with the active stripe overgrown by thick low-loss semiconductor cladding. This design gives rise to very similar losses for several lateral modes. In fact, most of the devices started lasing at a higher-order lateral mode. In comparison, in the recent study of broad-ridge QCLs with lossy metal sidewalls leading to larger losses for high-order lateral modes [20], multilateral mode operation was observed, but no indication of phase coherence was found.

We consider the simplest possible model for the dynamics of the transverse modes in QCLs which still includes the effect of phase-sensitive nonlinear mode coupling. The material gain is modeled as a two level medium. The fast relaxation times for population inversion, $T_1 \sim 1$ ps, and polarization, $T_2 \sim 0.1$ ps, characteristic of QCLs with a vertical laser transition, allow us to adiabatically eliminate both variables. The gain saturation is considered as a perturbation, truncated at the third order, which corresponds to the $\chi^{(3)}$ approximation. Since we have a large number of interacting and overlapping longitudinal modes as seen in the experimental spectra, we employ the mean-field approximation by averaging the field equations over the propagation direction z and including mirror losses into the total losses. We will get rid of this approximation later. The resulting equation for the complex time-dependent amplitude of the jth waveguide mode has the following form:

$$\frac{da_j}{dt} + (\kappa_j + i\Delta_j)a_j = g_j\Gamma_j a_j - \frac{g_j}{I_s}\sum_{k,l,m} G_{jklm} a_k a_l^* a_m, \quad (1)$$

where $\Gamma_j = \int_{AR} \varepsilon E_j^2 dA$ and $G_{jklm} = \int_{AR} \varepsilon E_j E_k E_l E_m dA$ are the normalized overlap integrals taken over the active region area, $g_j = 2\pi\omega_0 d^2 N_p T_2/(\hbar\mu_j^2)$ is the small-signal material gain, $I_s = \hbar^2/(d^2 T_1 T_2)$ is the saturation intensity. Δ_j, μ_j, and κ_j are the frequency detuning from the transition frequency, modal refractive index, and the modal loss, respectively; d is the dipole moment of the laser transition and N_P is the population inversion supported by pumping in the absence of lasing. The indices j, k, l, m run over all the included modes. The transverse distributions of the electric field $E_j(x, y)$ for the waveguide modes were calculated by the finite element method (COMSOL) and were used for far-field mode fitting and for calculating Γ_j, G_j, Δ_j, and κ_j.

The second term on the right-hand side of Eq. (1) describes a phase-sensitive nonlinear coupling between different modes which can lead to their frequency and phase locking. This process competes with the effect of waveguide dispersion and losses described by the complex detunings [the second term on the left-hand side of Eq. (1)].

We solve the resulting system of coupled nonlinear differential equations Eqs. (1) numerically. The initial conditions for the amplitudes are taken as a large set of randomly distributed complex amplitudes, with magnitudes of the order of 10^{-4} of steady-state lasing values. The equations are integrated until the amplitudes reach the steady state provided the latter exists. We defined detunings in the mean-field model as separations between closest longitudinal modes belonging to different transverse modes (about 0.04 meV).

An example of the dynamics of amplitudes and phases for three lateral modes is presented in Fig. 2. The nonlinear interaction leads to frequency pulling; as a result, frequencies of the lateral modes merge into a single frequency and the phase differences between the modes remain constant. This is clear from Fig. 2(b), in which the slope of the phase is the frequency detuning. Experimentally this effect should lead to merging of three combs belonging to

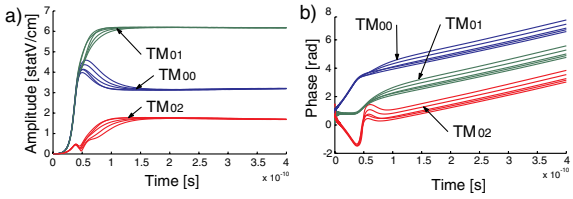

FIG. 2 (color online). Time-dependent dynamics of modal amplitudes of the electric field (in CGS units) (a) and total phases (b) for five random initial conditions. The gain is 3.5 times the threshold gain for the TM_{01} mode, which has the lowest threshold $g_{th} \sim 1.37 \times 10^{11}$ s^{-1} (about 15 cm^{-1}).

different transverse modes into a single comb, while the far-field pattern shows the presence of all three transverse modes with locked phases. The phase difference between the modes determines the radiation pattern.

To investigate the laser behavior as a function of injection current, we repeated the same time-dependent simulations starting from a random set of initial conditions for a broad range of gain values. For each value of the gain, the simulations continued until all *stable* steady-state solutions locked to a single frequency and constant phase difference were found. The results are plotted in Fig. 3.

According to the figure, there exists an intermediate range of gains where only one stable solution exists with all three modes locked to a single frequency. Outside this region there are two stable steady-state solutions which have different sets of amplitudes and lock to different frequencies. Note that one of these two solutions consists of only two nonzero modes (TM_{00} and TM_{02}). The two boundaries of the single-stability region are the points of a supercritical Hopf bifurcation describing appearance of the second stable lasing state. In the narrow vicinity of each boundary, there is a region where multiple solutions exist depending on the initial conditions. In this region the laser is expected to randomly hop from pulse to pulse between different mode patterns, which could result in the broadening of the spectrum. Qualitatively, these findings are well supported by the experimental measurements in Fig. 1 which show the synchronization of lateral mode combs within the certain range of currents and strong broadening of the spectra at currents in the vicinity of the synchronization regime.

Now we make an assumption which is in a sense opposite to the mean-field approximation adopted above. We assume that the longitudinal dependence of the electric field corresponds to the standing wave modes in a cold lossless cavity, $\propto \sin(N_j \pi z/L_c)$, where L_c is the cavity length and N_j is an integer number of the order of 1800 for our lasers. This approximation neglects any z dependence of modal amplitudes and carrier diffusion along z that would smear out the population inversion gratings imposed by the standing waves. The equations for the complex amplitudes Eqs. (1) of cold cavity modes remain of the same form, only the modal index becomes a double index counting both transverse and longitudinal modes. Also, the overlap integrals G_{jklm} now have to be taken over the cavity volume. These integrals contain the product of four sines with different arguments, so they are nonzero only for certain values of the longitudinal indices. Therefore, in this approximation the nonlinear interaction between modes is strongly reduced.

A sketch of spectral location of frequencies of cold cavity modes is schematically shown in Fig. 4(a). The spectrum can be split into the triplets where each triplet consists of longitudinal modes that belong to different lateral modes and have different longitudinal indices. The separation between the modes within each triplet is determined by the geometry of the cavity [20]. The lateral modes interact most efficiently when the overlap integral corresponding to the four-wave mixing process within each triplet is nonzero. The interaction is weaker than in the mean-field approximation because many four-wave mixing paths between the modes become forbidden. Nevertheless, simulations show that frequency and phase coupling is still possible.

Figure 4(b) shows the result of solving modified Eqs. (1) when each of the three lateral modes consists of five longitudinal modes, resulting in five triplets. The frequency separation of the cold modes within each triplet is about 2 times smaller than the distance $\hbar c\pi/(n_{\text{eff}} L_c) \sim 0.1$ meV between neighboring longitudinal modes belonging to one lateral mode. The gain is above the threshold for synchronization. In Fig. 4(b) the dynamics of the total phases of all 15 modes is shown. After the initial time of the order of the inverse growth rate of laser oscillations (~ 10 ps, not resolved in the figure), frequencies of the three modes forming each triplet become locked to a single frequency for all initial conditions. As a result, three combs merge into a single comb. In this case of well separated triplets the evolution of modes constituting a single triplet is practically the same no matter how many triplets we included in the modeling. This allows us to consider the dynamics of only one triplet.

We solved Eqs. (1) to find the time evolution of three complex amplitudes $a_j(t) = A_j(t)\exp[i\Phi_j(t)]$ forming a single triplet for each gain value starting from a large set of random initial conditions to the final time much longer

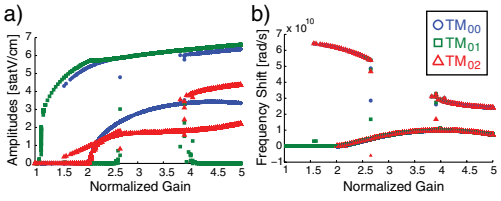

FIG. 3 (color online). Modal field amplitudes (a) and frequencies (b) of stable frequency- and phase-locked steady-state solutions as a function of small-signal gain g_j, normalized to g_{th}.

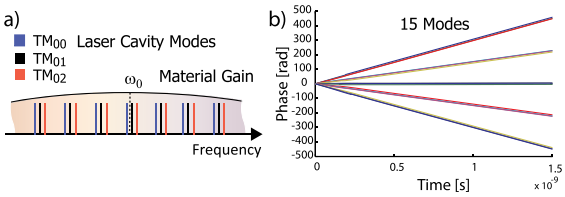

FIG. 4 (color online). (a) A sketch of spectral positions of cold cavity modes in the case of three lateral modes. (b) evolution of total phases of 15 modes (3 lateral modes times 5 longitudinal modes) for the gain 3.5 times laser threshold, which shows that three combs belonging to three lateral modes merge into a single comb.

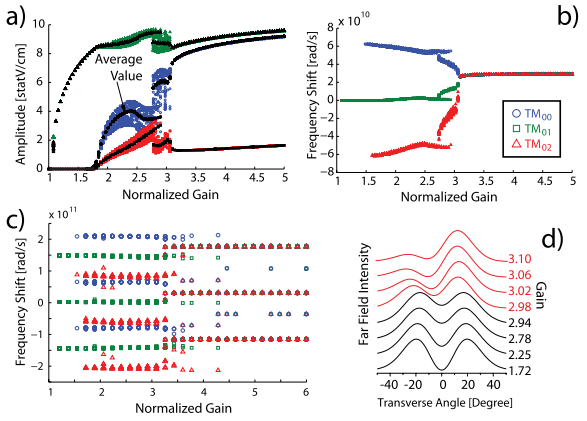

FIG. 5 (color online). (a) Absolute values of the amplitudes and (b) frequencies of the three modes forming a single triplet as a function of the linear gain normalized to the threshold value, calculated for a large set of random initial conditions. (c) Same as in (b) but for three closely spaced triplets, or three longitudinal modes per each lateral mode. (d) normalized far-field distribution for a single triplet at different gains (curves are shifted for clarity).

than the times of all transient processes. The result is shown in Figs. 5(a) and 5(b), where each point corresponds to the solution for a particular initial condition and gain. At gains higher than 3 times the laser threshold value, synchronization occurs with all three modes in the triplet locking to the same frequency. At lower gains, each mode lases at its own frequency and experiences slow amplitude and frequency modulation at the beat frequencies. The vertical spread of points around the average values in Fig. 5(a) corresponds to the amplitude of modulation in $A_j(t)$, whereas the frequency of the jth mode at gains below 3 in Fig. 5(b) is defined as the linear slope $\Omega_j = d\Phi_j(t)/dt$ averaged over time to remove slow frequency modulation. Figure 5(d) shows the far-field distribution which clearly demonstrates beam steering above synchronization threshold.

We also investigated the situation when the separation between neighboring triplets is 2 times smaller than the separation between neighboring modes within a triplet. In this case one should expect better agreement with the mean-field model due to stronger coupling between modes. We performed simulations for three overlapping triplets (nine modes) starting from 30 randomly distributed initial amplitudes and phases of each mode at each value of the gain. The results are shown in Fig. 5(c). Each point in Fig. 5(c) corresponds to a modal frequency Ω_j for a particular initial condition. There are two isolated intervals of gain around gain values 4 and 5 where the three triplets merge into three single peaks and the synchronized lasing state exists. Outside these intervals laser modes remain unlocked. The disappearance of the synchronization at higher gains is in agreement with the mean-field model and experimental data.

In conclusion, our modeling and experimental results reveal a new dynamic regime of the complete synchronization of multiple lateral modes in QCLs, in which the phases of these modes become locked and their combs merge into a single comb. Synchronization originates from four-wave mixing interaction in the active region of QCLs. This regime is accompanied by a strong beam steering effect.

This work was supported in part by NSF grants ECS-0547019 and EEC-0540832 (MIRTHE ERC). The Harvard authors acknowledge partial financial support from the Air Force Office for Scientific Research (AFOSR Grant No. FA9550-08-1-0047).

*belyanin@tamu.edu

[1] A. Pikovsky, M. Rosenblum, and J. Kurths, *Synchronization: A Universal Concept in Nonlinear Sciences* (Cambridge University Press, Cambridge, England, 2001).
[2] *Handbook of Chaos Control*, edited by E. Schöll and H. G. Schuster (Wiley-VCH, Weinheim, 2008), 2nd ed.
[3] L. Illing, D. Gauthier, and R. Roy, Adv. At. Mol. Opt. Phys. **54**, 615 (2006).
[4] J. Acebron, L. Bonilla, C. Perez-Vicente, F. Ritort, and R. Spigler, Rev. Mod. Phys. **77**, 137 (2005).
[5] A. Buehlmann and G. Deco, PLoS Comput. Biol. **6**, e1000934 (2010).
[6] T. Danino, O. Mondragon-Palomino, L. Tsimring, and J. Hasty, Nature (London) **463**, 326 (2010).
[7] Y. Khanin, *Principles of Laser Dynamics* (Elsevier, Amsterdam, 1995).
[8] C. Wang *et al.*, Phys. Rev. A **75**, 031802 (2007).
[9] C. R. Menyuk and M. A. Talukder, Phys. Rev. Lett. **102**, 023903 (2009).
[10] C. Y. Wang *et al.*, Opt. Express **17**, 12929 (2009).
[11] N. Yu *et al.*, Phys. Rev. Lett. **102**, 013901 (2009).
[12] P. Mandel and M. Tlidi, J. Opt. B **6**, R60 (2004).
[13] K. Otsuka, S.-C. Chu, C.-C. Lin, K. Tokunaga, and T. Ohtomo, Opt. Express **17**, 21 615 (2009).
[14] K. Wiesenfeld, S. Peles, and J. Rogers, IEEE J. Sel. Top. Quantum Electron. **15**, 312 (2009).
[15] W. Bewley, J. Lindle, C. S. Kim, I. Vurgaftman, J. Meyer, A. Evans, J. S. Yu, S. Slivken, and M. Razeghi, IEEE J. Quantum Electron. **41**, 833 (2005).
[16] N. Yu *et al.*, IEEE Trans. Nanotechnol. **9**, 11 (2010).
[17] L. K. Hoffmann, M. Klinkmüller, E. Mujagić, M. P. Semtsiv, W. Schrenk, W. T. Masselink, and G. Strasser, Appl. Phys. Lett. **92**, 061110 (2008).
[18] D. Allen, T. Sargent, J. Reno, and M. Wanke, IEEE J. Sel. Top. Quantum Electron. **17**, 222 (2011).
[19] S. Fathololoumi *et al.*, Opt. Express **18**, 10036 (2010).
[20] N. Stelmakh, M. Vasilyev, F. Toor, and C. Gmachl, Appl. Phys. Lett. **94**, 013501 (2009).